Pergamon

Geochimica et Cosmochimica Acta, Vol. 68, No. 11, pp. 2405–2415, 2004

0016-7037/04 $30.00 + .00

doi:10.1016/j.gca.2003.08.023

Porosity and fluid velocities in the upper continental crust (2 to 4 km) inferred from injection tests at the Soultz-sous-Forêts geothermal site

Luc Aquilina,[1,2,*] Jean-Raynald de Dreuzy,[2] Olivier Bour,[2] and Philippe Davy[2]

[1]BRGM—Service Eau, BP 6002, F-45060 Orléans cedex 02, France
[2]CAREN—Géosciences Rennes, UMR 6118 CNRS–Univ. Rennes1, Campus Beaulieu F-35042 Rennes cedex, France

(*Received February* 19, 2003; *accepted in revised form August* 29, 2003)

Abstract—A heat exchanger was created at the French Hot Dry Rock geothermal site using a doublet of boreholes at a depth of 3600–3800 m. After hydraulic stimulation, this exchanger was tested during a long-term circulation trial from July to November 1997. Tracer tests were carried out during the circulation trial.

An analysis of the tracers indicates a connected porous volume in the range of 0.5 to 2.5 $\times$ 10^6 m^3, with a connected porosity of the order of 0.9 to 2.3%. These values are one order of magnitude higher than values obtained by extrapolation from petrophysical investigation of the boreholes. This result is interpreted as being due to the connection of the major faults to a dense network of 2^{nd}-order structures.

Fluid circulation velocities inferred from the tracer test are of the order of 0.25 to 0.36 m/h. Velocities derived from observation of the migration of fresh fluids after injection into the granite during stimulation tests are of the same order of magnitude (0.02 to 0.17 m/h), yielding hydraulic conductivity estimates of 6.6 10^{-8} to 2.3 10^{-6} m/s^{-1}. Both the pressure gradient during the circulation test and the density gradient are related to freshwater injection, and can be considered as possibly equivalent to temperature and hydraulic gradients in the Rhine graben, at least during some specific geological events such as the Alpine uplift phases. Thus, the test shows that fluid migration can occur in the upper continental crust exhibiting "reservoir" properties, and these should be taken into account in large-scale modelling. These properties are in good agreement with a proposed scenario of evolution involving active fluid migration during the Eocene (Alpine uplift phase). It also supports the hypothesis of seawater-derived saline fluids stored in old fractured shield rocks, which implies deep seawater circulation in the continental crust.

1. INTRODUCTION

Circulation of meteoric fluids or injection of fluids originating from sedimentary basins in crystalline rocks of the upper continental crust (0.5–15 km) is suggested by several indirect lines of evidence such as metal deposits or fault filling (Fyfe, 1987; McCaig, 1988; Cathles, 1990; Torgersen, 1991; Marquer and Burkhard, 1992; Muchez and Sintubin, 1998), deep seismic profiles (Oliver, 1990), fluid movements related to earthquakes (Kerrich et al., 1987; Muir-Wood and King, 1993) or mobilization of fluid along mountain belts (Bethke and Marshak, 1990; Oliver, 1990; Ge and Garven, 1994; Huenges et al., 1997; Muchez et al., 2000). Finally, several authors have suggested the movement of continental fluids in subduction zones at depths of several kilometers (Kastner et al., 1991; Aquilina et al., 1997a). Over the last 30 yr, direct fluid systems in basements have been investigated all over the world. Scientific exploration programs such as Deep Geology of France or KTB (Boulègue et al., 1990; Aquilina et al., 1997c; Möller et al., 1997; Lodemann et al., 1998), and research carried out for waste storage (Frape and Fritz, 1987; Nurmi et al., 1988; Nordstrom et al., 1989a,b; Bottomley et al., 1990, 1994; Grimaud et al., 1990; Pearson et al., 1991; Beaucaire et al., 1999; Louvat et al., 1999) have shown that a fluid phase is omnipresent in the continental crust down to great depths. Because of thorough water-rock interaction, the origin of the fluids is still a matter of debate. However, there is growing evidence for a marine (or sedimentary) origin for such fluids (Pauwels et al., 1993; Muchez et al., 1995; Savoye et al., 1998; Beaucaire et al., 1999; Bottomley et al., 1999; Aquilina et al., 2000, 2002, 2003; Barth, 2000; Gleeson et al., 2000; Kloppmann et al., 2002). Such an origin implies downward fluid migration on a large scale. Nesbitt and Muehlenbachs (1995) suggested meteoric fluid convection in the top 10 km of the crust, but we still have only a poor understanding of the hydrogeological regimes that produce such circulation and the real hydraulic properties of the upper crust.

The circulation of fluids in an igneous basement is made possible through fractures in the low-porosity rocks. Depending on the interconnectivity of fractures forming continuous networks, fractured rocks range from very impervious (in nonconnected networks) to very permeable (in connected networks) (Bour and Davy, 1999; de Dreuzy et al., 2001a,b). In one example, at a research site for a nuclear waste laboratory in France (Vienne), boreholes have intersected fractures, and this has allowed fluid circulation leading to the abandonment of the site. The observation of fluids in fault zones of the deep basement has brought up the question of the reservoir properties of the basement, in particular the permeability and porosity of the rocks at different scales. At some of the investigated sites, local permeabilities have been measured in cores (Evans et al., 1997), and permeability has been derived from hydrogeological tests (Banks et al., 1996; Stober, 1997). However, we have little idea of the porosity at the scale of the crust, or the velocities of past and present fluid circulation. This question is

* Author to whom correspondence should be addressed at CAREN—Géosciences Rennes (luc.aquilina@univ-rennes1.fr).

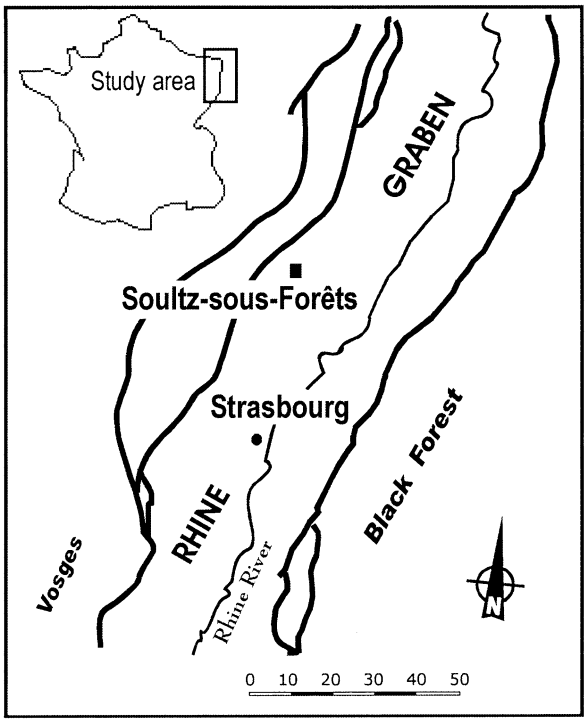

Fig. 1. Location map.

important since it forms the basis of large-scale hydrogeological models in which many parameters remain undetermined (Pribnow and Schellschmidt, 2000).

Geothermal research on Hot Dry Rocks (HDR) has also led to the investigation of subsurface rock properties (Aquilina et al., 1997b; Edmunds et al., 1984, 1985; Grigsby et al., 1983, 1989). Soultz-sous-Forêts (Rhine Graben, France; Fig. 1) is the French site of the European HDR program (Kappelmeyer et al., 1991). Two boreholes have been drilled at this site (between 1992 and 1994) in the granitic basement to a depth of 3600 and 3800 m (GPK-1 and GPK-2, respectively). These were hydraulically stimulated to create a heat exchanger at depth (Baria et al., 1999c). The present study presents estimates of the porosity of the granitic medium and the fluid velocity in the granitic basement. Values are inferred on the scale of a few km using the results of injection/production tests carried out between 1993 and 1996, and a long-term circulation test carried out between the two deep boreholes from July to November 1997.

2. GEOLOGICAL SETTING AND CIRCULATION TEST

The Soultz site is located on the west side of the Oligocene Rhine Graben (Fig. 1), on a thermal anomaly that has long been recognized (Benderitter and Elsass, 1995). The graben has a NNW-SSW-trending structure developed along faults extending more than 300 km on either side of the Graben. The Graben has an East-West asymmetric structure. It is filled by Tertiary deposits attaining a thickness of ~1.5 km in the West and 6 km in the East. The evolution of the area began during the Eocene, with major rifting and subsidence in Oligocene times (Western European Cenozoic rift system). The Soultz site is located on the western side of the Graben, on a horst structure covered by 1.4 km of sediments (mainly Triassic sandstones and Oligocene clay). The granite below the sedimentary cover is a Visean porphyroid granite with K-feldspar megacrysts (Genter and Traineau, 1992). It has undergone an early pervasive alteration (especially, replacement of biotite and plagioclase by chlorite) and several phases of alteration related to fluid circulation, expressed as fracture filling.

The heat exchanger at Soultz comprises two boreholes, GPK-1 and GPK-2, respectively attaining depths of 3.6 and 3.8 km (Fig. 2). The Soultz borehole open-hole sections are located in the granite below the sedimentary cover. An exploratory well (EPS-1) was also drilled in 1990 and cored from 930 m to 2227 m. The fractures and petrographic facies have been described by Genter and Traineau (1996). The faults are mainly grouped into two sets striking roughly N-S and dipping westward and eastward (N005 and N170, 70°W and 70°E) (Genter and Traineau, 1992, 1996; Sausse, 2002). The most common type of structure (95.5%) corresponds to sealed fractures, which are subdivided into minor and major sealed fractures. (1) Minor sealed fractures are filled with hydrothermal products and have a width < 1 mm. (2) Major sealed fractures are filled by hydrothermal products deposited during several hydrothermal stages. They have a width of > 1 mm, with an average value of 2.4 mm. (3) About 30 open fractures have also been observed in EPS-1 (less than 1% of the total number of fractures observed). They correspond to hydrothermal filled fractures with aperture in the central part of the fillings (quartz

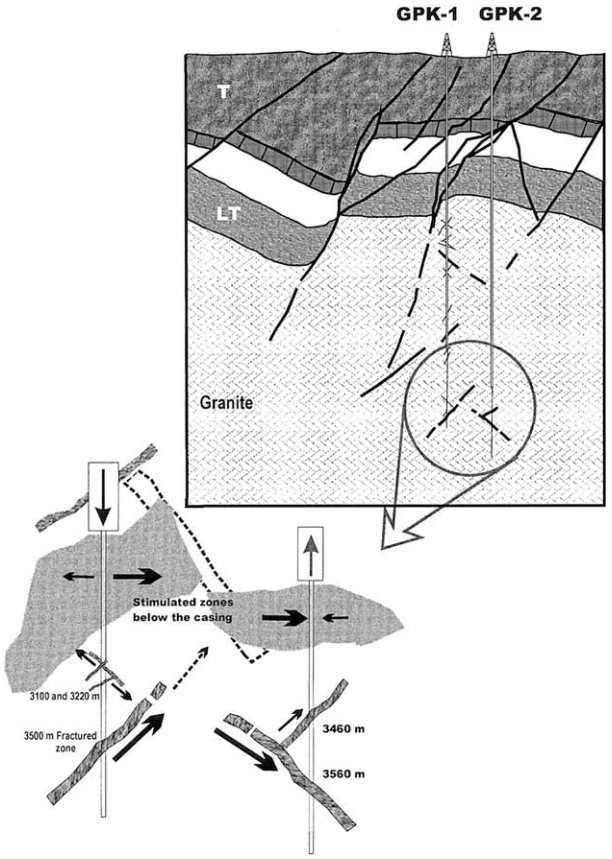

Fig. 2. Sketch of heat exchanger during the last test in 1997. T = Tertiary; LT = Lower Triassic.

Table 1. Flux distribution in the injection and production boreholes—1997 circulation test.

GPK-1 (injection)			
Beginning		End	
Depth range	Flux %	Depth range	Flux %
2860–2950	65	2860	50
		2880–2950	15
3100/3220	20	3220	22
3500	15	3500	13
GPK-2 (production)			
Depth range			Flux %
3200–3350			65
3460			27
3560			08

crystallization). The thickness of the fractures can reach 250 mm with a residual opening of 2–5 mm. These open fractures are also associated with wall-rock alteration and increased residual porosity. The fractures are not randomly distributed throughout the granitic section. Low-fracture density zones (<1/m) alternate with high-density zones (10–40/m). About 10 zones of high fracture density are observed between 1530 and 2230 m. The thickness of these altered zones varies from several metres to 20 m. The major fractures and the open fractures are associated with these zones. The thickest open zones are termed "fractured zones" in the following. Petrographic observations indicate a pervasive alteration of the whole granite as well as vein alteration related to the fractures. The fractured zones correspond to intense hydrothermal alteration with replacement of the granite minerals by white micas and clay minerals, with precipitation of quartz and carbonates (Ledésert et al., 1993; Genter and Traineau, 1996). Such fractured zones have great lateral extent and correspond to the occurrence of megascopic faults seen at the scale of the Rhine Graben. Geochemical logging of the drilling fluids, as well as monitoring of He and Rn (Aquilina and Brach, 1995b), shows that permeable zones correspond to some of the fractured zones (Aquilina and Brach, 1995a). Saline fluids (100 g/L) circulate within these permeable fractured zones (Pauwels et al., 1993; Aquilina et al., 1997b). Such zones have been identified at several depths: 1820, (2820), 3500 m in GPK-1, 2200 m in GPK-2 (no monitoring could be carried out deeper in this borehole). The frequency of such fractured zones is of the order of less than 1 per km and does not seem to decrease with depth.

The heat exchanger at Soultz is made up of two boreholes, GPK-1 and GPK-2, at depths of 3.6 and 3.8 km, respectively (Fig. 2), with a separation of 450 m at depth. Open-hole sections are located at 2850–3590 and 3210–3876 m, respectively. During the production and injection tests, flow logs measured the fluid production from the permeable zones or the injection of fluids into the permeable zones. The distribution of fluxes is given in Table 1. The main permeable zones in GPK-1 are located as follows (1) below the casing foot between 2850 and 2950 m, (2) a second minor zone at a depth of 3100–3220 m, (3) a fractured zone at 3500 m depth. The first zone results from stimulation with fresh water (high-pressure injection) carried out in 1993, which opened fractures situated mainly just below the casing foot. The second zone represents two fractures whose permeability had been enhanced by stimulation. The third zone corresponds to a major fractured zone, which created the main permeability of the open-hole before stimulation (Baria et al., 1999b). The fracture zone 1 located immediately below the casing at 3500 m can be considered as a "natural" system. A major zone in borehole GPK-2 is located below the casing, distributed over a greater depth interval than in GPK-1 and extending from 3200 down to 3360 m. Two fractures at depths of 3400 and 3560 m were also active. The upper zone results from stimulation, whose effects were observed mainly below the casing as also seen in GPK-1. During the 1997 circulation test, the upper zones below the casing in GPK-1 and GPK-2 corresponded to the main injection and production zones (65% of the total flux at the beginning of the test). During the 1997 test in the injection well, a reorganization of the fluxes presented in Table 1 was followed by a major drop in the injection pressure at constant flow rate (from 40–20 bars; Baria et al., 1999a).

Several injection/production tests were carried out in GPK-1 and GPK-2 from 1993 to 1997.

(1) After drilling of the GPK-1 borehole (Oct.–Dec. 1992), two stimulation tests were carried out in September and October 1993 and a total volume of 44300 m^3 of fresh water was injected (max. 36 L/s). The well was briefly vented shortly after each test (1100 and 650 m^3, respectively). The borehole was also vented several times for technical reasons between 1993 and 1996: December 1993 (production test), June 1994 (production test), November-December 1994 (production of drilling fluids for drilling of GPK-2), June 95 (short circulation test), and September-October 1996 (production of fluids for stimulation of GPK-2).

(2) In 1996, a stimulation test was carried out in GPK-2 (max. 80 L/s). More than 34000 m^3 (mainly fresh water) were injected into GPK-2, followed by production of slightly more than 10,000 m^3.

(3) A long-term circulation test between the two boreholes was carried out during the summer of 1997. The fluids were circulating at the surface within a gas-tight closed pipe system. Fluid pressures were maintained at 1.0–1.2 MPa to avoid degassing and consecutive precipitations. The circulation was maintained almost continuously during a 4-month period (July–November) at a rate of 21 to 25 kg/s (244,000 tonnes produced) with the temperature increasing slightly from 138 to 142°C (Baumgärtner et al., 1998; Baria et al., 1999a).

3. GEOCHEMICAL MONITORING TECHNIQUES AND INJECTION OF TRACERS

All the injection/production tests carried out at the Soultz site have been geochemically monitored (Aquilina and Brach, 1995a). During the 1997 long-term circulation test, 2–4 fluid-samples were collected daily. These fluids were analyzed on site for the following physicochemical parameters: pH, Eh, temperature, conductivity and dissolved oxygen. Silica, Ca and Cl contents were also determined. Tracer tests were carried out during the long-term circulation test in 1997, and their characteristics are summarized in Table 2. Tracers mixed with various volumes (6–11 m^3) of fresh water were injected into the whole

Table 2. Characteristics of the 1997 tracer tests.

Tracer	Mass injected (kg)	Volume of tracer solution (m^3)	Concentration in solution (g/L)	Concentration in injection line (g/L)
SF_6	0.163	11	0.0149	$1.85\ 10^{-3}$–$0.9\ 10^{-3}$
Benzoic Ac.	292	6.2	47.4	2.26
Fluorescein	150	6.2	27.3	1.06
Deuterium (D_2O)	44.4	$40\ 10^{-3}$	pure	167–206

open-hole section of the injection well (Table 2). Deuterium was injected downhole using a dump bailer just above the large fracture zone at 3500 m to mark a specific flow path (Vaute et al., 1998).

Fluorescein was determined on site with a fluorometer (detection limit 50 μg/L, uncertainty 15%) and further analyzed in the BRGM laboratories in Orléans using a spectrofluorometer ($\ll$1 μg/L, uncertainty 2%). Benzoïc acid was measured by high performance liquid chromatography $\ll$10 μg/L; uncertainty 2%] after separation on resin columns. Deuterium was analyzed by mass spectrometry at the laboratories in Orléans. All the samples were duplicated, and analyses were repeated at least twice for those having the highest values. Uncertainty is 0.8‰. SF_6 analyses were carried out by M. Gardiner (AEA Tech. Plc) using a gas chromatograph with EC detector. Further details about analytical procedures can be found in a BRGM report (Vaute et al., 1998).

4. RESULTS OF THE CHEMICAL MONITORING AND TRACER TESTS

4.1. Stimulation Test of GPK-1 and GPK-2

It is interesting to note that the stimulation tests (high-pressure injection) tests can be compared with tracer tests within a single well (push-pull tests) where fresh water is a natural tracer. The main characteristics of the injection-backflow tests in September and October 1993 are reflected in the fresh-water/brine ratio, defined from the Cl content determined after each injection test. This ratio dropped immediately after the casing was flushed out, falling to less than 95% of fresh water. After the casing was flushed in September, it decreased regularly down to 88% during the production of 1100 m^3. In October, the percentage of fresh water was ~85% after a production of 600 m^3. Similar results were observed after the 1996 injection test. Although a large volume of fresh water was injected, we observed a relatively rapid decrease of the percentage of fresh water recovered in the mixture produced after injection. The 1993 injection test was followed by several short production episodes (1993 to 1996), during which we measured the percentage of fresh water contained in the well. The evolution of this percentage with time is presented in Figure 3 (black squares). We also measured the freshwater content in the fluids produced after the stimulation test in 1996. The evolution of the freshwater content in the fluids produced from GPK-2 was also monitored throughout the circulation test in 1997. The evolution of the freshwater percentage between 1996 and 1997 is also plotted in Figure 3, with the 1996 stimulation tests used as the initial reference time (it is superimposed onto the evolution observed after the 1993 tests). There is a considerable change of the percentage during the 1996 test as well as between the 1996 and 1997 tests (Fig. 3).

4.2. Long-Term Circulation Test (1997)

In Figure 4, we present the return curves for the tracers normalized to the injection concentration (concentration in the injection flow line). First arrival times, derived from the breakthrough curves (Fig. 4), do not show any major differences between the tracers, with travel times converging to 70–80 h. A notable exception is deuterium, which is first detected 24 h after injection (Fig. 4). Fluorescein and benzoic acid show a fairly similar pattern with a maximum peak occurring between ~144 and 240 h. Both breakthrough curves have long flat tails, characteristic of tracer flow in heterogeneous systems but, due to recycling effects, the rate of decrease in concentration slows down towards the end of the test. The breakthrough curve for deuterium shows a completely different pattern, partly because deuterium was injected only at depth. The curve shows two distinct increases. At first, the curve rises simultaneously with fluorescein and benzoic acid to form a minor peak with a normalized concentration (C/Co) close to 0.001 (P1 in Fig. 4). A second much more significant peak (C/Co $>$ 0.003) is observed ~430 h after injection (P2 in Fig. 4), while no significant increase in other tracers is noticed at this time. The benzoic acid and fluorescein peak at 144–240 h correlates with the main flow path between the two boreholes. This main flow

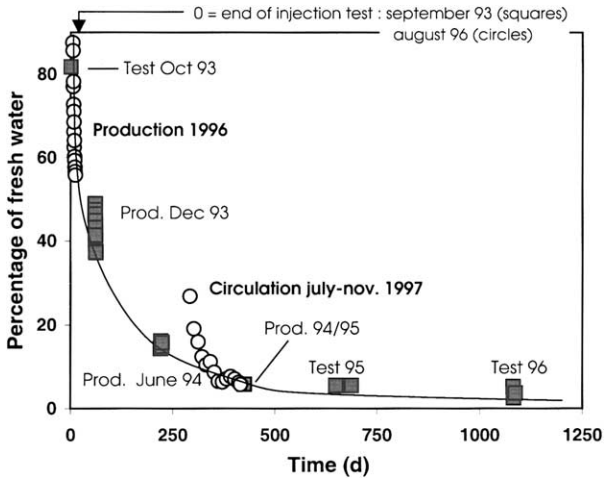

Fig. 3. Evolution of the percentage of brine in the fluids produced after large injection tests (1993 and 1996). Squares = evolution after 1993 stimulation (44,300 m^3 of fresh water injected into GPK1); circles = evolution after 1996 stimulation (34,000 m^3 of fresh water injected into GPK2)

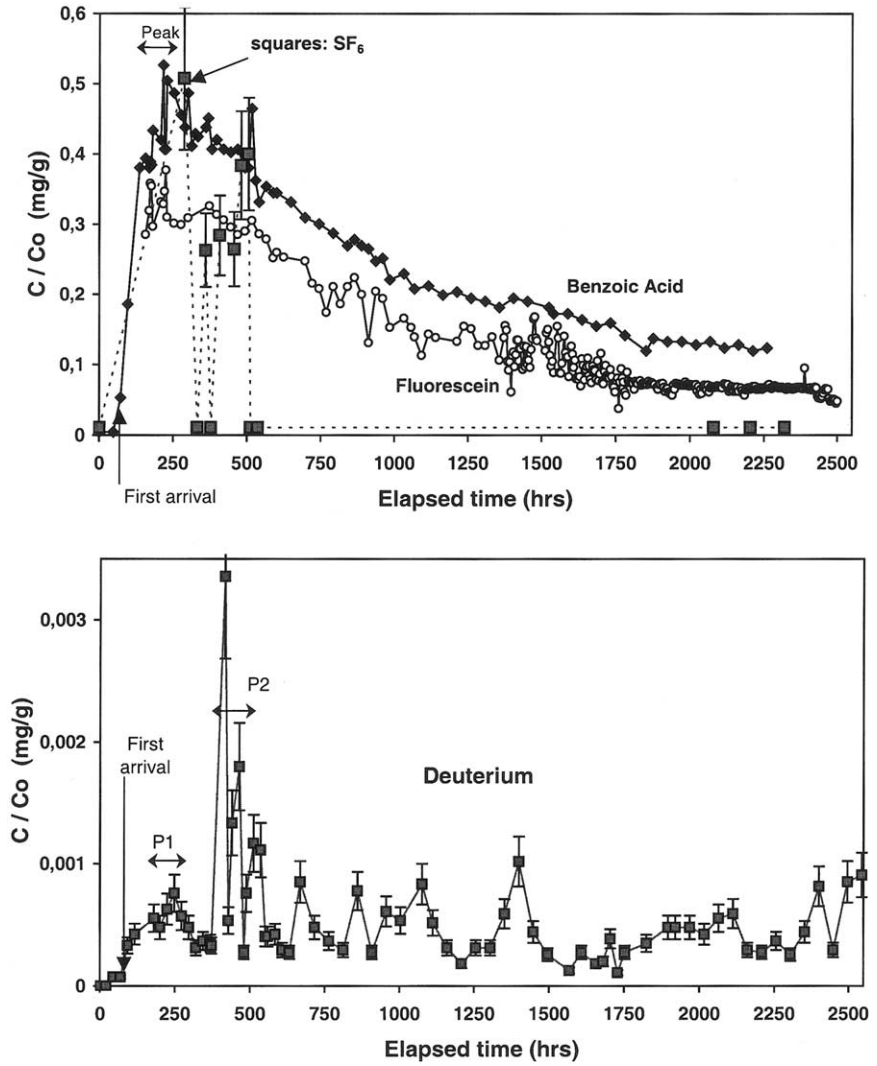

Fig. 4. Restitution curves, circulation test, 1997.

path absorbed and produced 65% of the flow, and is related to the fractured zones below the casing (2850–2950 in GPK-1; 3200–3360 in GPK-2) that were enhanced by stimulation. The high deuterium peak (430 h) is related to the specific flow path of the 3500-m-deep fracture zone where deuterium was injected. The poorly documented SF_6 curve shows a pattern that is comparable to the deuterium variation i.e., a sharp peak followed by an important and rapid decrease of the concentration, which then drops below the detection limit after 500 h.

5. DISCUSSION

5.1. Porous Volume of the Reservoir

Tracer tests are an important tool for estimating reservoir porous volume (i.e., connected porous volume), although tracer return time is related to both dispersion and adsorption. Dispersion is related to the heterogeneity of the medium, while adsorption is directly related to the contact surface between rock and fluid. Thus, neither of these phenomena is directly related to the porous volume, which itself represents a volume percentage of the whole rock volume. Despite this, the relatively constant concentration of the tracer after several cycles nevertheless allows estimation of the porous volume. This constant (or slowly decreasing) concentration suggests that the "reservoir" present between the two boreholes is a closed system (whatever the nature of the medium). Otherwise, a continuous decrease should be observed related to continuous addition of water from the external parts of the system (Rose and Adams, 1994; Rose and Apperson, 1997). In the case of a closed system, the porous volume is simply defined as the ratio of the tracer mass to the tracer constant concentration.

$$V_c = M/C_t, \quad (1)$$

where

V_c = connected porous volume,
M = mass of tracer injected, and
C_t = concentration of tracer reduced to a constant value due to recycling

Table 3. Reservoir volume computed from stabilised concentration of tracers (1997).

	Tracer mass (kg)	Stabilized conc. (mg/L)	Porous volume (Mm^3)
Benzoic acid	292	0.25	1.16
Fluorescein	150	0, 1	1.5
D_2O	44.4	0.1–0.02	0.5–2.2
SF_6	0.1635	Below detection	V > 10

Table 3 presents the volume computed from the different tracers during the 1997 circulation test.

Benzoic acid and fluorescein volumes are in the same order of magnitude: 1.2 to 1.5 10^6 m^3 (Table 3), which gives a good confidence to this order of magnitude. The deuterium estimate is less precise due to large fluctuations in concentration but could be in the same order of magnitude. Deuterium is potentially more affected than other tracers by dispersion effects because it is a small molecule. Although Becker and Shapiro (2000) described experiments at the Mirror Lake site showing no difference between deuterium and pentafluorobenzoic acid, higher dispersivities have been demonstrated at other fractured sites (Garcia-Gutierrez et al., 1997; Himmelsbach et al., 1998). We find no significant difference between fluorescein, benzoic acid or deuterium behavior in the Soultz circulation test. The SF_6 concentrations below the detection limit after 500 h gives a minimum value for the porous volume that is clearly higher than other tracers. Results of SF6 and deuterium tracers suggest that benzoic acid and fluorescein concentrations did not reach stability, which could lead to underestimation of the porous volume. Although SF_6 has previously been used as a geothermal tracer (Upstill-Goddard and Wilkins, 1995), the relatively sparse measurements and possible evolution of the samples yield results with less confidence than other tracers.

The order of magnitude of the porous volume of the fracture-connected network can also be estimated from petrographic investigations of the granite. The computation is based on the following steps: (1) calculating the thickness of the permeable fracture planes intersected in the boreholes, (2) extrapolating the fractures as planes connecting the two boreholes. This allows us to extrapolate the 1-D observation in the borehole to a 3-D volume between the boreholes within which fluids circulate during the injection tests. The porous volume can be determined using three dimensions, one of them being defined as the cumulative thickness of the opened fractures in the borehole (Fig. 5). This cumulative thickness represents all the apertures by which fluids injected into the borehole can penetrate the granitic medium. The cumulative thickness is defined from observations of the cored section of borehole EPS-1 (2200 m depth, close to GPK-2), which provide the thickness of the opened fractures (Genter and Traineau, 1992; Genter and Traineau, 1996) and from geophysical logging of GPK-1 and GPK-2 boreholes which allow us to observe such structures. As observed in the flow logs during the 1997 test (Table 1), the flow in GPK-1 is mainly confined to i) “natural” zones at 3100–3220 and 3500 m, ii) an upper stimulated zone at 2860–2950. The “natural” zones have a permeable cumulative thickness estimated (by analogy to EPS-1 structures) to range from 0.2 to 0.5 m (Genter and Traineau, 1996; Sausse, 2002). Their cumulative thickness is made up of (1) an opened fractured zone at 3500 m (0.005–0.025 m), (2) opened fractures at 3100–3220 m (0.005–0.05 m), (3) porous wall-rocks (0.2–0.4 m; Ledésert, 1993). Although the stimulated zone at 2860–2950 m (below the casing) is less constrained, its cumulative permeable thickness can be estimated to range between 0.25 and 1.5 m by taking into account a fracture density range of 10 to 30 fractures per metre and using the density measured in borehole EPS-1 (Genter and Traineau, 1996). All the fractures are considered to be opened in the stimulated zone (2860–2950 m). We assume an opening of 0.5 to 1 mm, which represents more than 60% of the fracture width in borehole EPS-1 (Genter and Traineau, 1996). The sum of estimations obtained for zones i and ii (0.45 to 2 m) defines the permeable thickness, i.e., the vertical thickness of the porous reservoir. A second dimension is given by the distance separating GPK-1 and GK-2 (450 m), while the third dimension is the most difficult to estimate. During stimulation tests, injection at high pressure created several thousand microseismic events that have been recorded. The width of the microseismic cloud observed during stimulation (Beauce et al., 1991) has provided a lateral limit (300 m).

Using the values defined above, the porous volume between the two boreholes ranges from 50,000 to 300,000 m^3. This estimation is one order of magnitude lower than the computation using tracer dilution during the 1997 tracer test (Eqn. 1). There are some uncertainties associated with the different values used in the computations. First, in the tracer computation, we assume a stabilized tracer concentration due to recycling. The tracer recovery time may be considered as too short to

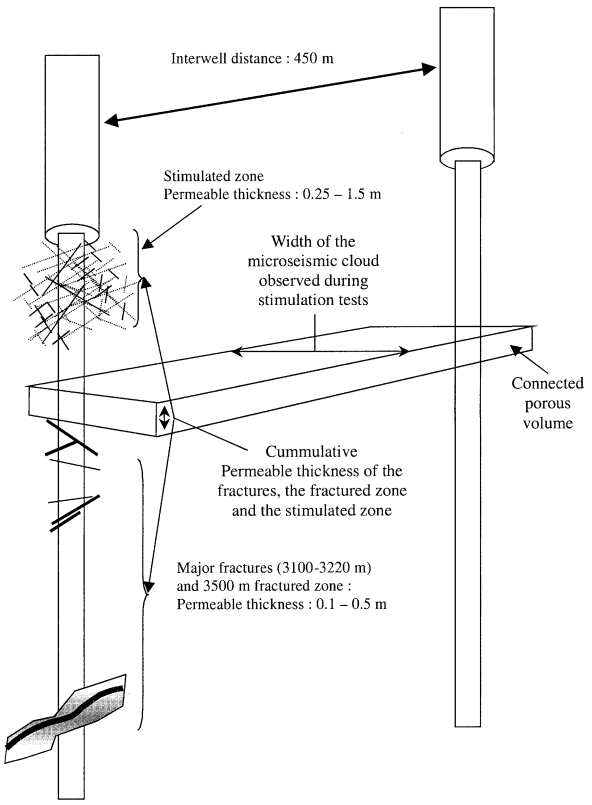

Fig. 5. Sketch of the connected porous volume and the reservoir volume between the two injection-production boreholes.

support this hypothesis. However, this uncertainty implies that the computed porous volume is a minimum estimate. Secondly, in the petrographic estimation, the limit taken for the width of the rock volume (300 m) is inferred from the microseismic cloud. This value represents a broad estimate of the microseismic cloud width. Although the origin of the microseismic events is a matter of debate, we consider that the cloud width corresponds to the major fluid circulation zone. Such a hypothesis is supported by the correlation between the microseismic cloud and the fluid injection and production zones in the boreholes. The difference between the extrapolation from borehole-observed porosity and the porous volume derived from the tracer test is attributed to two levels of heterogeneity of the fractured medium. (1) The permeable fractures are not continuous between the boreholes but should be seen as a complex network involving several fractured zones that do not necessarily intercept the borehole, thus defining a larger volume than the cumulative thickness used. Such connections are indicated by the presence of deuterium in the upper connected zone although this tracer was directly injected into the 3500 m fracture. Thus, the actual porous volume is higher than the extrapolation of the intersection between the fracture network and the borehole, as observed in the boreholes from coring and logging. This suggests that the extrapolation from 1-D to 3-D is not as simple as the hypothesis used in estimating the petrographic porous volume. (2) The fractured zones include several scales of fracturing and thus different porosities. As presented in the geological section, at least three scales of fracture thickness have been identified (Genter and Traineau, 1996): large fractured zones (several metres), major fractures (several millimeters) and numerous thin fractures (<1 mm). Regarding the larger fractured zones and major fractures as first-order structures, the second-order fractures were initially impermeable and were only reactivated during the stimulation. Along with these second-order fractures, we can define a microporosity through the microfissures and mineral joints connected to the second-order fractures, thus defining a third order of discontinuity. Neither of these orders of fracture were taken into account in the petrographic estimation.

The connected porosity of the rock volume defined between the two boreholes can be estimated from the previous computations of the porous volume of the reservoir: it is given by the ratio between the porous volume and the total rock volume (open-hole height x interwell distance x seismic cloud width). Using volume estimates obtained from petrographic studies, the connected porosity varies from 0.05 to 0.3%, while it varies from 0.9 to 2.3% using tracer estimates (except SF_6). The difference between these two estimates is attributed to the development of a second-order porosity generated by stimulation of the granitic medium (not taken into account in petrographic observations) and underestimation of the fracture network density due to the one-dimensional observation of the borehole. The highest values compare more closely with values in the literature (Nordstrom et al., 1989b; Savoye et al., 1998), although the scale of investigation is different.

5.2. Fluid Velocities

Geochemical tracers allow the estimation of fluid velocities in the fractured granite during the test, i.e., under strongly influenced conditions. Different values of time lapse can be defined (Table 4). (1) The shortest time is defined as the first arrival in GPK-2 after injection in GPK-1, i.e., the first sample showing a tracer concentration above the detection limit. This time ranges from 70 to 95 h. (2) A second time is defined through the maximum tracer concentration, which shows a peak appearing after 144–240 h after injection of fluorescein and benzoic acid and after 430 h for deuterium. (3) A mean time is defined using the barycenter of the breakthrough curve. The times obtained in this way are divided by the travel distance. Since the distance used is the interwell distance (450 m), the velocities are apparent velocities (although these are true velocities and not Darcy velocities). The highest velocity and the peak velocity can be defined using benzoic acid and fluorescein tracers, thus representing the transfer conditions in the upper zone. In the case of deuterium, these computations can be performed for the lower zone. For benzoic acid and fluorescein, we can determine the order of magnitude of the mean velocity.

Table 4. Fluid velocities in the granite-1997 circulation test (m/h).

	Benzoic acid	Fluorescein	Deuterium
V_{max} (first arrival time)	6.6	—	4.9
V_{peak} (major peak arrival between 144–240 h)	1.8–1.35	2.2–1, 8	1.6
$V_{2nd\ peak}$ (deuterium peak arrival 430 h)			1.0–0.9
V_{mean} (mean arrival time)	0.36–0.25		0.45–0.30

The velocities computed from the tracer test can also be compared with estimates based on the evolution of the fresh water to brine ratio with time (Fig. 3). On Figure 3, we can see that, after each stimulation, the mixing evolves towards the initial concentration of the natural brine (i.e., fresh water free mixing), but the rate of change decreases with time. This evolution takes place without involving any movement other than natural fluid circulation in the granite reservoir. Circulation during the 1997 test seems to have a limited effect on the chloride concentration compared with the evolution between 1996 and 1997, due to recycling between the two boreholes. Figure 3 shows that, after 1 yr, the fresh water injected in 1993 or 1996 is no longer present in the fluids produced. The injected fresh water has a much lower density than the natural brine once at the temperature of the reservoir. This density contrast causes the fresh water to rise in the permeable granite zones. Within the space of 1 yr, the injected volume of fresh water is almost completely removed from the vicinity of the boreholes. As discussed above, the assumed stimulated rock volume is defined from the microseismic event cloud (300 m wide in an E-W direction and 750 m length on either side of the borehole in a N-S direction) and the open-hole section height. We assume that the fresh water has at least traveled out of this volume, which thus defines a minimum distance. Using this volume and a time scale on the order of 1 yr, we obtain an estimated velocity ranging from 0.02 to 0.17 m/h. These velocities are similar to the mean velocities derived from the circulation test (0.25 to 0.45 m/h), although the values obtained from the tracer tests are higher. The similarity between the mean velocities during the test and those inferred from fluid migration are in agreement with (1) the relatively low pressures

necessary for circulation without any loss; (2) the circulation observed once the boreholes were closed between the upper and the lower fractured zones (3.5 L/s). All these points indicate that the fluid movement is relatively rapid in the granite.

The velocities allow us to estimate the hydraulic conductivity of the granitic medium. The hydraulic conductivity is simply defined through Darcy's law:

$$Q = K \times \Delta h/\Delta L \quad (2)$$

with

$$Q = V_{mean} \times \phi$$

where

- Q = fluid flux per unit surface (Darcy's velocity)
- K = hydraulic conductivity(m/s)
- V_{mean} = mean velocity defined (1) from the tracer tests (0.25–0.36 m/hr), (2) from the salinity change (0.02–0.17 m/h)
- ϕ = porosity defined from tracer tests (0.9–2.3%)
- Δh = pressure difference (addition of injection pressure and production pressure, 45–60 b)
- ΔL = inter-well distance (450 m)

The hydraulic conductivity obtained ranges from $4.6\ 10^{-7}$ to $2.5\ 10^{-6}$ m/s (the range corresponds to the uncertainty of the computation) using the tracer test velocities, and from $3.7\ 10^{-8}$ to $1.2\ 10^{-6}$ m/s (the range corresponds to the uncertainty of the computation) using the velocities based on salinity evolution. Such hydraulic conductivities are one to two orders of magnitude higher than values inferred from well testing in fractured granites at a depth higher than 1 km (Clauser, 1992; Banks et al., 1996; Stober, 1997), and several orders of magnitude higher than the hydraulic conductivity derived from KTB measurements (Huenges et al., 1997). However, they remain in the range of fractured granite close to the surface (Clauser, 1992; Banks et al., 1996; Stober, 1997). Due to the depth of measurement, the values at Soultz should compare more closely to KTB measurements. However, a crucial factor at Soultz is the presence of fractured zones that are clearly responsible for a large part of the permeable properties of the granite. Although, stimulation has enhanced the natural permeability of the medium, it is thought that the increase is mainly related to the development of the connection of the borehole to the main natural fractured zones (Murphy et al., 1999). While hydraulic stimulation has a major effect on the impedance of the boreholes, it has a more limited effect on the permeability of the medium inferred from the tests. Permeability is enhanced by a factor of 20 after the major stimulations, while flux is increased by only one order of magnitude (Baria et al., 1999b). Thus, we consider that natural hydraulic conductivities reaches the higher values observed from well testing or one order of magnitude lower, i.e., in the range 10^{-8}–10^{-9} m/s. Such values are several orders of magnitude higher than values used in modelling of the Rhine graben when integrating the granite as a whole (Clauser and Villinger, 1990; Pribnow and Schellschmidt, 2000) but they are in good agreement with values allowing convection in the fault system of the Rhine Graben (Bächler et al., 2003), although in that case, the thickness of the fractured zones is assumed to be 200 m. Another effect may be related to the scale dependence of permeability, since the scale of the Soultz test is several orders of magnitude higher than core measurements or single borehole tests.

The high velocities observed may be attributed to the density disturbance induced by injection. However, the very large temperature gradient in the graben might also cause driving forces similarly to the density gradient. The pressure differential between the injection and production borehole pressures (sum of the injection and production pump pressures) varied during the circulation test between 45 and 60 bars. The order of magnitude of the test gradient can be attained in natural systems. For example, this is the case in the Rhine graben where the gradient between the Schwarzwald and the Rhine river may be only ~15 times lower than in the Soultz test. During orogenic phases, high relief can be created that produces gradients as high as those used during the 1997 test. This could have been the case during the Eocene-Oligocene period, at the beginning of the graben evolution. From chemical and isotopic studies of fluids in the graben, Aquilina et al. (2000) described the variation of the fluid composition and migration in the graben as a succession of phases with different hydrogeological regimes and water-rock interaction conditions. The beginning of the Oligocene is thought to correspond to the period of fluid introduction into the granite. The results of the tracer tests suggest that, due to the hydraulic gradient and/or thermal gradient, natural circulation in the granite might have been rather rapid, at least during some specific tectonic events. These data support the possibility of marine and/or sedimentary fluid migration at great depth in the basement during specific geological episodes. Bethke and Marshak (1990) described sedimentary fluid migration induced by tectonic activity as the "plate tectonics of groundwater." Geological events may be related to fluid infiltration down to several km depth in the basement, which leads the concept of groundwater geodynamics. Because water is an intrinsic component of the crust (Deming, 1994), phases of fluid migration are directly related to geodynamic evolution and could thus be used to "trace" specific episodes of tectonic activity.

6. CONCLUSION

Tracers have circulated in the porous volume defined by fractured zones occurring between the two boreholes at the Soultz-sous-Forêts Hot Dry Rock site, at a depth of 2850 to 3800 m. Several tracers were injected during a long-term circulation test. From the tracer test, we can estimate a connected porous volume of the order of more than 1 million m^3. This volume is about one order of magnitude greater than the volume estimated from petrographic and geophysical investigations of the boreholes. This suggests that the porosity of the fractured zones observed in the boreholes is a first-order phenomenon, and at least another order of smaller fractures contributes to the flow in the granitic medium. Flow logs during the test, and microseismic monitoring during injection tests, allow us to determine the circulating volume. From this volume, we obtain a global connected porosity ranging between a low value of 0.05–0.3% and a high value of 0.9–2.3%.

The characteristics of the long-term circulation test (1997) show maximum apparent velocities of 6.6 m/h and mean apparent velocities of 0.25–0.45 m/h. The variation in the per-

centage of fresh water contained in the fluids after heavy stimulation tests shows that the injected fluids have migrated in the granite during the years of investigation. Velocities derived from this observation are of the same order as the mean velocities derived from the long-term circulation test, which allows us to determine a hydraulic conductivity range of 6.6 10^{-8} to 2.3 10^{-6} m/s^{-1}. This result indicates that a pressure gradient of 45 to 60 bars—or a density gradient—is able to drive rapid circulation in the granite at great depth. It is thought that the temperature and hydraulic gradients existing in the Soultz granite are likely to induce a density gradient allowing rapid natural fluid migration in the granite.

The results of the chemical monitoring of the Soultz experiments carried out between 1993 and 1997 have allowed the investigation of some properties of a fractured granitic medium in the depth range of 3–4 km. Although the porosity/permeability has been enhanced by hydraulic stimulation of the granitic medium, most of the properties are similar to those in natural fractured and altered Hercynian granites. The experiments confirm that the upper continental crust exhibits reservoir properties, i.e., (1) nonnegligible connected porous volumes, of the order of a few percent of the total volume; (2) natural velocities in such environments may be of the order of 1 km/yr. Our study indicates that fluid transfer in the granite (Aquilina et al., 2000) might have been an active process at depths of 3–4 km at specific geological periods. It also supports the possibility of marine infiltration in the basement, thus reflecting the response of fluids to geological evolution.

Acknowledgments—The Soultz field work was carried out in the framework of a BRGM Research project. Facilities on site were provided within the framework of the European Hot Dry Rock Project (DG XII) with the help of the coring team (A. Gérard, R. Baria, J. Baumgärtner and S. Kleber). M. Brach, L. Vaute, E. Jacquot and P. Deschamps are thanked for the field work. Part of the work was performed within the framework of the European SALTRANS contract EVK1-CT-2000-00062. Andrew McCaig, Judith Sausse, Peter Sak and associate editor Eric Oelkers are thanked for detailed comments that greatly helped to clarify the manuscript. M. S. N. Carpenter postedited the English style. The first author is also indebted to J. S. Bach (cello cantatas) for musical support during the long nights of data interpretation.

Associate editor: E. H. Oelkers

REFERENCES

Aquilina L. and Brach M. (1995a) Characterization of Soultz hydrochemical system: WELCOM (Well Chemical On-Line Monitoring) applied to deepening of GPK-1 borehole. *Geotherm. Sci. Technol.* **4**(4), 239–251.

Aquilina L. and Brach M. (1995b) WELCOM: Evolution of chemical monitoring of drilling fluids and industrial perspectives. *SPE Drilling Completion* **Sept. 95,** 158–164.

Aquilina L., Dia A., Boulègue J., Bourgois J., and Fouillac A. M. (1997a) Geochemistry of fluid and solid samples from convergent margin off Peru: Implications for fluid circulation within subduction zones. *Geochim. Cosmochim. Acta* **61,** 1233–1245.

Aquilina L., Pauwels H., and Fouillac C. (1997b) Water-rock interaction processes in the Triassic sandstone and the granitic basement of the Rhine graben: Geochemical investigation of a geothermal reservoir. *Geochim. Cosmochim. Acta* **61**(20), 4281–4295.

Aquilina L., Sureau J. F., Steinberg M., and team G. (1997c) Comparison of surface, aquifer, and pore waters form a Mesozoïc sedimentary basin and its underlying Paleozoïc basement, Southeastern France: Chemical evolution of waters with diagenesis and relation ship between aquifers. *Chem. Geol.* **138,** 185–209.

Aquilina L., Genter A., Elsass P., and Pribnow D. (2000) Evolution of fluid circulation in the Rhine Graben: Constraints from the chemistry of present fluids. In *Hydrogeology of Crystalline Rocks* (eds. I. Stober and K. Bucher). Kluwer. pp. 177–203.

Aquilina L., Ladouche B., Doerfliger N., Seidel J. L., Bakalowicz M., Dupuy C., and Le Strat P. (2002) Origin, evolution and residence-time of saline thermal fluids (Balaruc springs, S-France): Implications for fluid transfer across the continental shelf. *Chem. Geol* **196,** 1–21.

Aquilina L., Ladouche B., Doerfliger N., and Bakalowicz M. (2003) Deep water circulation, residence time, and chemistry in a karst complex. *Ground Water,* **41**(3), p. 790–805.

Bächler D., Kohl T., and Rybach L. (2003) Impact of graben-parallel faults on hydrothermal convection—Rhine Graben case study. *Phys. Chem. Earth* **28,** 431–441.

Banks D., Odling N., Skarphagen H., and Rohr-Torp E. (1996) Permeability and stress in crystalline rocks. *Terra Nova* **8,** 223–235.

Baria R., Baumgärtner J., Gérard A., and Jung R. (1999a) Results of the long term circulation test. Socomine Internal Report.

Baria R., Baumgärtner J., Gérard A., Jung R., and Garnish J. (1999b) European HDR research programme at Soultz-sous-Forêts (France) 1987–1996. *Geothermics* **28,** 655–669.

Baria R., Baumgärtner J., Gérard A., Reinhard J., and Garnish J. (1999c) European HDR research programme at Soultz-sous-Forêts (France) 1987–1996. *Geothermics* **28,** 655–669.

Barth S. R. (2000) Geochemical and boron, oxygen and hydrogen isotopic constraints on the origin of salinity in groundwaters from the crystalline basement of the Alpine Foreland. *Appl. Geochem.* **15,** 937–952.

Baumgärtner J., Gérard A., Baria R., Jung R., Tran-Viet T., Gandy T., Aquilina L., and Garnish J. (1998) Circulating the HDR reservoir at Soultz: Maintaining production and injection flow in complete balance. In *Program and Abstracts of the 23rd Workshop on Geothermal Reservoir Engineering,* pp. 26–28. Stanford University.

Beaucaire C., Gassama N., Tresonne N., and Louvat D. (1999) Saline groundwaters in the hercynian granites (Chardon Mine, France): Geochemical evidence for the salinity origin. *Appl. Geochem.* **14,** 67–84.

Beauce A., Fabriol H., Le Masne D., Cavoit C., Mechlerand P., and Chen X. (1991) Seismic studies on the HDR site of Soultz-sous-Forêts (Alsace, France). *Geotherm. Sci. Technol* **3,** 239–266.

Becker M. W. and Shapiro A. M. (2000) Tracer transport in fractured crystalline rock: Evidence of nondiffusive breakthrough tailing. *Water Resources Res.* **36**(7), 1677–1686.

Benderitter Y. and Elsass P. (1995) Structural control of deep fluid circulation at the Soultz HDR site, France: A review. *Geotherm. Sci. Technol.* **4,** 227–237.

Bethke C. M. and Marshak S. (1990) Brine migration across North America—The plate tectonics of groundwater. *Annu. Rev. Earth Planet. Sci.* **18,** 287–316.

Bottomley D. J., Gascoyne M., and Kamineni D. C. (1990) The geochemistry, age, and origin of groundwater in a mafic pluton, East Bull Lake, Ontario, Canada. *Geochim. Cosmochim. Acta* **54,** 933–1008.

Bottomley D. J., Gregoire D. C., and Raven K. G. (1994) Saline groundwaters and brines in the Canadian shield: Geochemical and isotopic evidence for a residual evaporite brine component. *Geochim. Cosmochim. Acta* **5,** 1483–1498.

Bottomley D. J., Katz A., Chan L. H., Starinsky A., Douglas M., Clark I. D., and Raven K. G. (1999) The origin and evolution of Canadian shield brines: Evaporation or freezing of seawater? New lithium isotope and geochemical evidence from the lave craton. *Chem. Geol.* **155,** 295–320.

Boulègue J., Benedetti M., Gauthier B., and Bosch B. (1990) Les fluides dans le socle du sondage GPF Sancerre-Couy. *Bull. Soc. Geol. France* **5,** 789–796.

Bour O. and Davy P. (1999) Clustering and size distributions of fault patterns: Theory and measurements. *Geophys. Res. Lett.* **26 (***13***),** 2001–2004.

Cathles L. M. (1990) Scales and effects of fluid flow in the upper crust. *Science* **248,** 323–329.

Clauser C. (1992) Permeability of crystalline rocks. EOS *Trans. Am. Geophys. Union* **73**(21), 233–237.

Clauser C. and Villinger H. (1990) Analysis of conductive and convective heat transfer in a sedimentary basin, demonstrated for the Rheingraben. *Geophys. J. Int.* **100,** 393–414.

de Dreuzy J. R., Davy P., and Bour O. (2001a) Hydraulic properties of two-dimensional random fracture networks following a power law length distribution: 1-Effecive connectivity. *Water Resources Res* **37 (*8*),** 2065.

de Dreuzy J. R., Davy P., and Bour O. (2001b) Hydraulic properties of two-dimensional random fracture networks following a power law length distribution: 2-Permeability of networks based on log-normal distribution of apertures. *Water Resources Res.* **37 (*8*),** 2079.

Deming D. (1994) Fluid flow and heat transport in the upper continental crust. In *Geofluids: Origin, Migration and Evolution of Fluids in Sedimentary Basins* **Vol. 78** (ed. J. Parnell), pp. 27–42. Geological Society.

Edmunds W. M., Andrews J. N., Burgess W. G., and Kay R. L. (1984) The evolution of saline and thermal groundwaters in the Carnmenellis granite. *Min. Mag.* **48,** 407–424.

Edmunds W. M., Kay R. L., and McCartney R. A. (1985) Origin of saline groundwaters in the Carnmenellis granite (Cornwal, England): Natural processes and reaction during hot dry rock reservoir circulation. *Chem. Geol.* **49,** 287–301.

Evans J. P., Forster C. B., and Goddard J. V. (1997) Permeability of fault-related rocks, and implications for hydraulic structure of fault zones. *J. Struct. Geol.* **19-11,** 1393–1404.

Frape S. N. and Fritz P. (1987) Geochemical trends from groundwaters from the Canadian shield. In *Saline Waters and Gases in Crystalline Rocks* **Vol. 33** (eds. P. Fritz and S.N. Frape), pp. 19–38. Geological Association of Canada.

Fyfe W. S. (1987) The fluid inventory of the crust and its influence on crustal dynamics. In *Saline Waters And Gases In Crystalline Rocks* **Vol. 33** (eds. P. Fritz and S. Frape), pp. 1–4. Geological Association of Canada.

Garcia-Gutierrez M., Guimera J., Yllera de Llano A., Hernandez-Benitez A., Humm J., and Saltink M. (1997) Field tracer experiment in a low permeability fractured medium: Results from El Berrocal site. *J. Contam. Hydrol.* **26,** 189–201.

Ge S. and Garven G. (1994) A theoretical model for thrust-induced deep groundwater expulsion with application to the Canadian rocky. *J. Geophys. Res.* **99,** 13851–13868.

Genter A. and Traineau H. (1992) Borehole EPS-1, Alsace, France: A preliminary geological results from granite core analyses for hot dry rock research. *Sci. Drill.* **3,** 205–214.

Genter A. and Traineau H. (1996) Analysis of macroscopic fractures in granite in the HDR geothermal well EPS-1, Soultz-sous-Forêts, France. *J. Volcanol. Geotherm. Res.* **72,** 121–141.

Gleeson S. A., Yardley B. W., Boyce A. J., Fallick A. E., and Munz I. A. (2000) From basin to basement: The movement of surface fluids into the crust. *J. Geochem. Explor.* **69-70,** 527–531.

Grigsby C. O., Tester J. W., Trujillo P. E., Abbot C. J., Holley C. E., and Blatz L. A. (1983) Rock-water interactions in hot dry rock geothermal systems: Field investigations of in situ geochemical behavior. *J. Volcanol. Geotherm. Res.* **15,** 101–136.

Grigsby C. O., Tester J. W., Trujillo P. E., and Counce D. (1989) Rock-water interactions in the Fenton Hill new Mexico, hot dry rock geothermal systems I Fluid mixing and chemical geothermometry. *Geothermics* **18,** 629–656.

Grimaud D., Beaucaire C., and Michard G. (1990) Modelling of the evolution of ground waters in a granite system at low temperature: The Stripa ground waters, Sweden. *Appl. Geochem.* **5,** 515–525.

Himmelsbach T., Hötzl H., and Maloszewski P. (1998) Solute transport processes in a highly permeable fault zone of Lindau fractured rock test site (Germany). *Ground Water* **36**(5), 792–800.

Huenges E., Erzinger J., and Kück J. (1997) The permeable crust: Geohydraulic properties down to 9191 m depth in the KTB borehole. *Geophys. Res. Lett.* **102,** 18 255–18265.

Kappelmeyer O., Gérard A., Schloemer W., Ferrandes R., Rummel F., and Benderitter Y. (1991) European HDR project at Soultz-sous-Forêts general presentation. *Gotherm. Sci. Technol.* **2**(4), 263–289.

Kastner M., Elderfield H., and Martin J. B. (1991) Fluids in convergent margins: What do we know about their composition, origin, role in diagenesis and importance for chemical fluxes? *Phil. Trans. R. Soc. Lond. Ser. A* **335,** 243–259.

Kerrich R., Kaminenei D. C., Borre D., Baldwin D. K., McLarty E., and Thivierge R. H. (1987) Cyclic deformation and chemical transport in the Folson lake fault zone, East Bull lake anorthosite-gabbro complex: Evidence for seismic pumping? *Appl. Geochem.* **2,** 103–126.

Kloppmann W., Girard J.-P., and Négrel P. (2002) Exotic stable isotope compositions of saline waters and brines from crystalline basement. *Chem. Geol.* **184,** 49–70.

Ledésert B. (1993) Fracturation et paléocirculations hydrothermales. Application au granite de Soultz-sous-Forêts. Ph.D. thesis. University of Poitiers.

Ledésert B., Dubois J., Genter A., and Meunier A. (1993) Fractal analysis of fracture applied to Soultz-sous-Forêts hot dry rock geothermal program. *J. Volcanol. Geotherm. Res.* **57,** 1–17.

Lodemann M., Fritz P., and Wolf M. (1998) On the origin of saline fluids in the KTB (Continental Deep Drilling Project of Germany). *Appl. Geochem.* **13**(5), 653–671.

Louvat D., Michelot J. L., and Aranyossy J. F. (1999) Origin and residence time of salinity in the Aspö groundwater system. *Appl. Geochem.* **14,** 917–925.

Marquer D. and Burkhard M. (1992) Fluid circulation, progressive deformation and mass-transfer processes in the upper crust: The example of basement-cover relationships in the External Crystalline Massifs, Switzerland. *J. Struct. Geol.* **14-8/9,** 1047–1057.

McCaig A. M. (1988) Deep fluid circulation in fault zones. *Geology* **16,** 867–870.

Möller P., et al.. (1997) Paleofluids and recent fluids in the upper continental crust: Results from the German continental deep drilling program (KTB). *J. Geophys. Res.* **102,** 18,233–18,254.

Muchez P. and Sintubin M. (1998) Contrasting origin of palaeofluids in a strike-slip fault system. *Chem. Geol.* **145,** 105–114.

Muchez P., Slobodnik M., Viaene W. A., and Keppens E. (1995) Geochemical constraints on the origin and migration of palaeofluids at the northern margin of the Variscan foreland southern Belgium. *Sediment. Geol.* **96,** 191–200.

Muchez P., Sintubin M., and Swennen R. (2000) origin and migration pattern of palaeofluids during orogeny: Discussion on the Variscides of Belgium and northern France. *J. Geochem. Explor.* **69-70,** 47–51.

Muir-Wood R. and King G. C. P. (1993) The impact of earthquakes on fluids in the crust. In *Geofluids: Origin, Migration and Evolution of Fluids in Sedimentary Basins* **Vol. 78** (ed. J. Parnell) p. 374. Geological Society.

Murphy H., Brown D., Jung R., Matsunaga I., and Parker R. (1999) Hydraulics and well testing of engineered geothermal reservoirs. *Geothermics* **28,** 491–506.

Nesbitt B. E. and Muchlenbachs K. (1995) Geochemical studies of the origins and effects of synorogenic crustal fluids in the southern Omineca Belt of British Columbia, Canada. *Geol. Soc. Am. Bull.* **107**(9), 1033–1050.

Nordstrom D. K., Ball J. W., Donahoe R. J., and Whittemore D. (1989a) Groundwater chemistry and water-rock interactions at Stripa. *Geochim. Cosmochim. Acta* **53,** 1227–1240.

Nordstrom D. K., Lindblom S., Donahoe R. J., and Barton C. (1989b) Fluid inclusions in the Stripa granite and their possible influence on the groundwater chemistry. *Geochim. Cosmochim. Acta* **53,** 1741–1756.

Nurmi P., Kukkonen I., and Lahermo P. (1988) Geochemistry and origin of saline groundwaters in the Fennoscandian shield. *Appl. Geochem.* **3,** 185–203.

Oliver J. (1990) COCORP and fluids in the crust. In *The role of fluids in crustal processes.* Studies in Geophysics. National Academy Press. pp. 128–139.

Pauwels H., Fouillac C., and Fouillac A. M. (1993) Chemistry and isotopes of deep geothermal saline fluids in the Upper Rhine Graben: Origin of compounds and water-rock interactions. *Geochim. Cosmochim. Acta* **57,** 2737–2749.

Pearson F. J., Balderer W., Loosli H., Lehmann B., Matter A., Peters T., Schmassmann H., and Gautschi A. (1991) Applied isotope hdrogeology: A case study in northern Switzerland. *Studies Environ. Sci.* **43**, 439 pp.

Pribnow D. and Schellschmidt R. (2000) Thermal tracking of upper crustal fluid flow in the Rhine Graben. *Geophys. Res. Lett.* **27**(13), 1957–1960.

Rose P. E. and Adams M. C. (1994) The application Rhodamine WT as a geothermal tracer. *Geotherm. Res. Council Trans.* **18,** 237–240.

Rose P. E. and Apperson K. D. (1997) Fluid volume and flow constraints for a hydrothermal system at Beowave, Nevada. In *Program and Abstracts of the SPE Annual Technical Conference. Soc. Petrol. Eng.*, SPE 38762.

Sausse J. (2002) Hydromechanical properties and alteration of natural fracture surfaces in the Soultz granite (Bas-Rhin, France). *Tectonophysics* **348,** 169–185.

Savoye S., Aranyossy J. F., Beaucaire C., Cathelineau M., Louvat D., and Michelot J. L. (1998) Fluid inclusions in granites and their relationships with present-day groundwater chemistry. *Eu. J. Mineral.* **10,** 1215–1226.

Stober I. (1997) Permeabilities and chemical properties of water in crystalline rocks of the Black Forest, Germany. *Aquat. Chem.* **3,** 43–60.

Torgersen T. (1991) Crustal scale fluid transport: Magnitude and mechanism. *Geophys. Res. Lett.* **18,** 917–918.

Upstill-Goddard R. C. and Wilkins C. S. (1995) The potential of SF6 as a geothermal tracer. *Water Res.* **29**(4), 1065–1068.

Vaute L., Aquilina L., Gentier S., Pinault J. L., and Rose P. (1998) *Tests de traçage réalisés sur le site géothermique de Soultz-sous-Forêts*. BRGM.